Temperature-Controlled Uptake and Release in PNIPAM-Modified Porous Silica Nanoparticles

Ye-Zi You,[†] Kennedy K. Kalebaila,[‡] Stephanie L. Brock,*[,‡] and David Oupický*[,†]

Departments of Pharmaceutical Sciences and Chemistry, Wayne State University, Detroit, Michigan 48202

Received November 27, 2007. Revised Manuscript Received March 10, 2008

Temperature-dependent uptake and release of small molecules within porous silica nanoparticles has been achieved by treatment of preformed, thiol-functionalized micro-to-mesoporous silica nanoparticles (MSN) with pyridyl disulfide-terminated poly(*N*-isopropylacrylamide) (PNIPAM−S−S−Py). The resulting nanoparticle−polymer composites show uptake and release of fluorescein at room temperature (below the lower critical solution temperature, LCST, of the polymer) and a low level of leakage at 38 °C (above LCST, <2% after 2 h). The data are consistent with a mode of action in which fluorescein diffusion occurs readily when the polymer is in the random coil conformation but is significantly retarded when the polymer adopts the globule conformation. This mode of action is opposite to that observed for systems in which the PNIPAM is grown from the porous silica surface or co-condensed with silica and is accompanied by a greater than 10-fold improvement in fluorescein retention in the "pore-closed" conformation.

Introduction

Of the M41S mesoporous silica materials, hexagonal MCM-41 and cubic MCM-48 have been of great interest because of their many attractive features, such as stable mesoporous structures, large surface areas, tunable pore sizes and volumes, good biocompatibility, and well-defined surface properties for subsequent organic functionalization.[1–4] M41S materials have been explored for many practical applications including catalysis, synthesis of optically active materials, polymerization, and separation technology.[1] Because the pore voids of this class of materials exhibit relatively narrow pore size distributions in the range of 1−4 nm, micro-to-mesoporous silicas can selectively host molecules of various sizes, shapes, and functionalities.[1] Accordingly, M41S-based materials are being investigated as passive molecular transporters.[5–10]

Recently, significant effort has been devoted to the development of "smart" mesoporous silica-based delivery systems in which uptake and delivery of molecules in the pore voids can be controlled at will by a variety of external stimuli. Thus, coumarin modification of MCM-41 allows photocontrolled release of guest molecules,[11,12] whereas chemically triggered release can be obtained with particles linked by reducible bonds to CdS or iron oxide nanoparticle "caps".[3,4] Likewise, redox- or pH-controlled nanovalves based on switchable rotaxane molecules permit ready opening and closing of the nanovalves by chemical means,[13–15] and ionically controlled molecular-gate-based modified MCM-41 enables the regulation of mass transport from the solution to the mesopores.[16] In most cases, effective use of these modified silica nanospheres is limited by the irreversibility of the pore opening (chemically bound caps) or the relative complexity of the synthesis of the molecular gates (reversible rotaxanes).

A simple and reversible delivery system can be envisioned based on a combination of porous silica nanoparticles with stimuli-responsive or "smart" polymers in which access to the pores is controlled by application of a stimulus, such as a change in pH, ionic strength, or temperature. Poly(*N*-isopropylacrylamide) (PNIPAM) represents one of the most widely investigated temperature-responsive polymers and exhibits a lower critical solution temperature (LCST, the temperature at which the polymer undergoes a change from

* To whom correspondence should be addressed. E-mail: oupicky@wayne.edu, sbrock@chem.wayne.edu.
[†] Department of Pharmaceutical Sciences.
[‡] Department of Chemistry.

(1) Stein, A.; Melde, B. J.; Schroden, R. C. *Adv. Mater.* **2000**, *12*, 1403–1419.
(2) Sayari, A.; Hamoudi, S. *Chem. Mater.* **2001**, *13*, 3151–3168.
(3) Lai, C.-Y.; Trewyn, B. G.; Jeftinija, D. M.; Jeftinija, K.; Xu, S.-A.; Jeftinja, S.; Lin, V. S.-Y. *J. Am. Chem. Soc.* **2003**, *125*, 4451–4459.
(4) Giri, S.; Trewyn, B. G.; Stellmaker, M. P.; Lin, V. S.-Y. *Angew. Chem., Int. Ed.* **2005**, *44*, 5039–5044.
(5) Azaïs, T.; Tourné-Péteilh, C.; Aussenac, F.; Baccile, N.; Coelho, C.; Devoisselle, J.-M.; Babonneau, F. *Chem. Mater.* **2006**, *18*, 6382–6390.
(6) Horcajada, P.; Rámila, A.; Pérez-Pariente, J.; Vallet-Regí, M. *Microporous Mesoporous Mater.* **2004**, *68*, 105–109.
(7) Muñoz, B.; Rámila, A.; Pérez-Pariente, J.; Díaz, I.; Vallet-Regí, M. *Chem. Mater.* **2003**, *15*, 500–503.
(8) Arruebo, M.; Galán, M.; Navascués, N.; Téllez, C.; Marquina, C.; Ibarra, M. R.; Santamaría, J. *Chem. Mater.* **2006**, *18*, 1911–1919.
(9) Izquierdo-Barba, I.; Martinez, A.; Doadrio, A. L.; Pérez-Pariente, J.; Vallet-Regí, M. *Eur. J. Pharm. Sci.* **2005**, *26*, 365–373.
(10) Lu, J.; Liong, M.; Zink, J. I.; Tamanoi, F. *Small* **2007**, *3*, 1341–1346.
(11) Mal, N. K.; Fujiwara, M.; Tanaka, Y. *Nature* **2003**, *421*, 350–353.
(12) Mal, N. K.; Fujiwara, M.; Tanaka, Y.; Taguchi, T.; Matsukata, M. *Chem. Mater.* **2003**, *15*, 3385–3394.
(13) Nguyen, T. D.; Tseng, H. R.; Celestre, P. C.; Flood, A. H.; Liu, Y.; Stoddart, J. F.; Zink, J. I. *PNAS* **2005**, *102*, 10029–10034.
(14) Nguyen, T. D.; Liu, Y.; Saha, S.; Leung, K. C.-F.; Stoddart, J. F.; Zink, J. I. *J. Am. Chem. Soc.* **2007**, *129*, 626–634.
(15) Leung, K. C.-F.; Nguyen, T. D.; Stoddart, J. F.; Zink, J. I. *Chem. Mater.* **2006**, *18*, 5919–5928.
(16) Casasús, R.; Marcos, M. D.; Martinez, Máñez.; Ros-Lis, J. V.; Soto, J.; Villaescusa, L. A.; Amorós, P.; Beltrán, A.; Guillem, C.; Latorre, J. *J. Am. Chem. Soc.* **2004**, *126*, 8612–8613.

10.1021/cm703363w CCC: $40.75
Published on Web 04/25/2008

a hydrated to a dehydrated state[17,18]) of ~32 °C in water.[19] Thus, at temperatures below the LCST, the polymer is in the coil (soluble) conformation, while above the LCST, it is in the globule or collapsed (insoluble) state. This property has been exploited in applications ranging widely from rheology modifications to drug delivery.[20,21]

Studies on mesoporous silica−PNIPAM hybrids are few. López and co-workers prepared hybrids by either conducting atom transfer radical polymerization (ATRP) of the NIPAM monomer from the surface of calcined MCM-41 treated with an initiator or cogelation of an aminopropylsilyl-terminated PNIPAM with silica in the presence of a surfactant template.[22,23] Both methods produce materials capable of fluorescein uptake and release above the LCST of PNIPAM (40−50 °C), and the latter method produced membranes capable of rejecting crystal violet at low temperatures. The data are consistent with a mechanism whereby the polymers are encapsulated within the pores of MCM-41, acting to reduce small molecule diffusion when in the open coil configuration while facilitating diffusion in the globule conformation by effectively retreating to the pore walls. However, these systems are very leaky at room temperature, releasing one-half to one-third of the quantity of fluorescein released at 40−50 °C after just 2 h, and the particles are very large (10−20 μm) and thus poorly dispersible.[22,23]

Herein, we present PNIPAM-modified micro-to-mesoporous silica nanoparticles (MSN) with sizes on the order of 100 nm prepared by chemical attachment of preformed polymer to preprepared porous particles. Importantly, these new materials show minimal leakage in the "closed" conformation (<2% release over 2 h vs >25% release in the López system[22]). These improvements appear to be related to a different mode of action than seen previously since the uptake and release in the presently reported system occurs above, rather than below, the LCST.

Experimental Section

Materials. Tetraethylorthosilicate (TEOS), 3-mercaptopropyltrimethoxysilane (MPTMS), *N*-cetyltrimethylammonium bromide (CTAB), 5,5′-dithiobis-2-nitrobenzoic acid (Ellman's reagent), *N*-isopropylacrylamide (NIPAM), 2,2′-azobisisobutyronitrile (AIBN), and 2,2′-dipyridyl disulfide (Aldrithiol-2) were all purchased from Aldrich and used as received. Nanopure water was dispensed from a Nanopure Diamond, Barnstead purification system.

Synthesis of 2-Dodecylsulfanylthiocarbonylsulfanyl-2-methyl Propionic Acid (DMP). 1-Dodecanethiol (20.2 g, 0.10 mol), acetone (58.0 g, 1.0 mol), and tricaprylylmethylammonium chloride (1.0 g, 0.0025 mol) were added into a flask and cooled to 0 °C under a nitrogen atmosphere. Sodium hydroxide solution (50%) (9.0 g, 0.11 mol) was added over a period of 10 min. After the mixture was stirred for an additional 20 min, carbon disulfide (7.6 g, 0.10 mol) in acetone (10.0 g) was added over 30 min, and the color turned gradually red. Chloroform (17.8 g, 0.15 mol) was added, followed by dropwise addition of 40 g of 50% sodium hydroxide solution over 20 min. The mixture was stirred overnight; then 200 mL of water was added, followed by 80 mL of concentrated HCl to acidify the aqueous solution. After removing organic solvents, the solid was filtered and then stirred in 300 mL of isopropanol. The insoluble solid was filtered off, leaving an isopropanol solution which was concentrated, and the resulting solid recrystallized from hexane to afford 12.0 g of product (yield 33%). ^{1}H NMR data: $CDCl_3$ (δ) 0.89 (t, 3H, $-C_{11}CH_{23}CH_3$), 1.2−1.47 (m, 18H, $-CH_2CH_2C_9H_{18}CH_3$), 1.68 (m, 2H, $-S-CH_2CH_2-C_{10}H_{21}$), 1.73 (s, 6H, $-S-C(CH_3)_2COOH$), 3.3 (t, 2H, $-S-CH_2-C_{11}H_{23}$), Supporting Information, Figure S1.

Scheme 1. Synthesis of Pyridyl Disulfide-Terminated PNIPAM

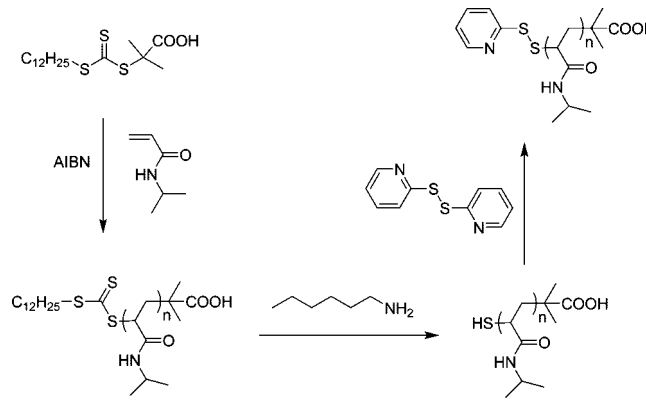

RAFT Polymerization of NIPAM To Produce PNIPAM−S−C−S)−S−$C_{12}H_{25}$. The temperature-responsive polymer, PNIPAM, containing a pyridyl disulfide end group was prepared via reversible addition fragmentation chain transfer (RAFT) polymerization in 3 steps (Scheme 1). Polymerization of 4.0 g of NIPAM with 120.0 mg of DMP was conducted in the presence of 4.0 mg of AIBN in 5.0 mL of DMF in a 20 mL vial. The vial was sealed and immersed in a preheated water bath at 60 °C. Polymerization was halted by immediate exposure to air and cooling with dry ice. The product was precipitated in ether, filtered, and dried at room temperature. PNIPAM−S−C(S)−S−$C_{12}H_{25}$ was characterized using a combination of size exclusion chromatography (SEC) and gel permeation chromatography.

Aminolysis of Trithiocarbonate-Terminated PNIPAM To Yield Thiol-Terminated PNIPAM. The trithiocarbonate-terminated PNIPAM (PNIPAM−S−C(S)−S−$C_{12}H_{25}$) was treated with hexylamine to yield thiol-terminated PNIPAM (PNIPAM-SH) as follows. A 3.0 g amount of trithiocarbonate-terminated PNIPAM in 5 mL of DMF was deoxygenated by a stream of nitrogen for 2 h. To that solution, 5 drops of $Na_2S_2O_4$ solution was added to prevent oxidation of the thiols to disulfides. This was followed by addition of 2.0 mL of hexylamine. The mixture was stirred at room temperature for another 12 h. The thiol-terminated PNIPAM (PNIPAM-SH) was obtained by pouring the mixture into ether and filtering and drying in vacuum at room temperature. The trithiocarbonate absorbance at 310 nm was absent from the UV spectrum of PNIPAM-SH (Supporting Information, Figure S2), consistent with conversion of trithiocabonate groups to thiol groups.

Preparation of Disulfide Pyridyl-Terminated PNIPAM. A solution containing 2.5 g of Aldrithiol-2, 1.0 mL of glacial acetic acid, and 20 mL of methanol was added to a 100 mL round-bottom flask with stir bar, followed by addition of PNIPAM-SH. After 24 h at room temperature, the reaction mixture was concentrated under

(17) de las Heras Alarcón, C.; Pennadam, S.; Alexander, C. *Chem. Soc. Rev.* **2005**, *34*, 276–285.
(18) Yerushalmi, R.; Scherz, A.; van der Boom, M. E.; Kraatz, H.-B. J. *Mater. Chem.* **2005**, *15*, 4480–4487.
(19) You, Y.-Z.; Hong, C.-Y.; Pan, C.-Y.; Wang, P.-H. *Adv. Mater.* **2004**, *16*, 1953–1957.
(20) Qiu, Y.; Park, K. *Adv. Drug Delivery Rev.* **2001**, *53*, 321–339.
(21) Kopecek, J. *Eur. J. Pharm. Sci.* **2003**, *20*, 1–16.
(22) Fu, Q.; Rao, G. V. R.; Ista, L. K.; Wu, Y.; Andrzejewski, B. P.; Sklar, L. A.; Ward, T. L.; López, G. P. *Adv. Mater.* **2003**, *15*, 1262–1266.
(23) Fu, Q.; Rao, G. V. R.; Ward, T. L.; Lu, Y.; López, G. P. *Langmuir* **2007**, *23*, 170–174.

vacuum and the concentrate added to 5.0 mL of THF. The disulfide pyridyl-terminated PNIPAM (PNIPAM−S−S−Py) was obtained by precipitating in ether, filtering, and drying in vacuum at room temperature. The presence of the pyridyl disulfide functionality was confirmed by ^{1}H NMR and UV−vis spectroscopy (Supporting Information, Figure S2). The molecular weight and PDI were determined by SEC (Supporting Information, Figure S3).

Synthesis of MSN-SH. Micro-to-mesoporous silica nanoparticles (MSN) functionalized with a thiol linker were synthesized by reaction of TEOS with MPTMS according to the procedure reported by Lin and co-workers.[3] The ratio [MPTMS]/[TEOS] in the reaction was 0.20. While Lin and co-workers appear to prepare MCM-41, Walcarius and co-workers note that ratios greater than 0.1 often lead to wormhole structures (MCM-48).[24] The chemically accessible thiol group surface coverage of the MSN-SH was estimated by treatment with Ellman's reagent. Ellman's reagent was prepared by dissolving 12 mg of reagent in 5 mL of buffer and kept in a freezer prior to use. In a typical analysis, 2.5 mg of the thiol linker was dissolved in 10 mL of Na_2HPO_4 buffer (pH 8.0), of which 1 mL of this solution was mixed with 1 mL of Ellman's reagent. Absorbance readings were taken at 412 nm ($\epsilon = 14\ 150\ cm^{-1}$ for Ellman's reagent) after 20 min of standing for the mixture, the blank (buffer solution), and the MSN-SH solution. The amount of free thiol in the 10 mL sample was calculated as described by Reiner and co-workers.[25]

Surface Modification of MSN with Temperature-Responsive Polymer. Thiol-functionalized MSN was reacted with PNIPAM−S−S−Py to prepare the desired MSN-PNIPAM. The reaction mixture contained a suspension of 0.10 g of MSN-SH in 20 mL of methanol, 0.5 mL of glacial acetic acid, and 2.0 g of PNIPAM−S−S−Py. The mixture was stirred for 24 h at room temperature followed by centrifugation at 4000 rpm to obtain the product, which was dried at room temperature under vacuum.

Characterization of MSN and MSN-PNIPAM Hybrids. Powder X-ray diffraction (PXRD) was used to study the crystallinity of the products using a diffractometer equipped with a rotating copper anode source. The data were collected over a range of $1.5° \leq 2\theta \geq 10°$ at the Max Planck Institute of Colloids and Interfaces in Germany. Particle sizes and the morphology of the materials were investigated by transmission electron microscopy (TEM) on a JEOL 2010F Analytical Electron Microscope at 200 kV. TEM samples were prepared by placing a drop of a sonicated acetone solution of MSN-SH or MSN-PNIPAM on a carbon-coated copper grid and then drying in a vacuum desiccator.

The surface area, average pore size, cumulative pore volume, and pore size distributions were determined from nitrogen adsorption/desorption isotherms acquired at 77 K using a 30 s equilibrium interval on an ASAP 2010 Micromeritics porosimeter. MSN-SH samples were degassed at 100 °C for 24 h and MSN-PNIPAM samples at 50 °C for 12 h, in order to remove any adsorbed molecules prior to the analysis. The surface area was computed using the BET (Brunauer−Emmett−Teller) model. The average pore size and cumulative pore volumes were obtained from the BJH (Barret−Joyner−Halenda) model.[26] The pore size distribution was obtained from density functional theory (DFT) modeling using the DFT package of the Micromeritics V2.00 software over the entire range of the adsorption isotherm.[5] Thermal gravimetric analyses (TGA) were collected on a Perkin-Elmer Pyris 1 TGA instrument, under a nitrogen atmosphere, at a heating rate of 5 °C/min.

Fluorescein Loading and Release Studies. The temperature-responsive loading of fluorescein in MSN-PNIPAM was achieved by vigorously stirring 110 mg of MSN-PNIPAM in a solution of fluorescein (4.0×10^{-6} M) in 10 mL of pH 7.4 phosphate-buffer solution (PBS) at room temperature for 24 h. Then, MSN-PNIPAM loaded with fluorescein was isolated by centrifugation at 4000 rpm, washed extensively with 50 °C deionized water 5 times to remove physiosorbed matter, and dried at 50 °C. All the washings were collected. The solution temperature was increased from room temperature to 38 °C, resulting in a precipitate that was filtered and washed with a PBS solution at 50 °C. The amount of fluorescein encapsulated was calculated from the difference in the concentration of the initial solution of fluorescein and that of the reaction medium combined with the subsequent washings. Release studies were conducted at 20 and 38 °C in PBS. In a typical release experiment, two vials containing the MSN-PNIPAM loaded with fluorescein (∼10.0 mg) and PBS solution (2.0 mL, pH 7.4) were kept at 25 or 38 °C, respectively. Aliquots were removed at specified time intervals over several days, and the absorbance was measured at 490 nm.

Control Experiments. Nonporous silica nanoparticles functionalized with a thiol linker were synthesized by a modified Stöber process using TEOS in ethanol as described by Rossi[27] and Rao.[28] The number of accessible thiol groups on the MPTMS-functionalized SiO_2-thiol was determined to be 13.1 mmol/g. PNIPAM−S−S−Py was grafted onto the nonporous silica particles as described for MSN. Loading and release experiments of the PNIPAM-modified dense silica spheres and thiol-functionalized mesoporous silica (MSN-SH) were conducted in a similar manner as for MSN-PNIPAM.

Determination of Phase Transition Temperatures. Determination of the phase transition temperature was performed using a ZetaPlus Particle Size analyzer (Brookhaven Instruments) equipped with 35 mW solid-state laser (658 nm). To determine the transition temperature, the temperature dependence of the scattering intensity at 90° from 1 mL of solution in a glass cuvette was measured. The temperature was increased by discrete temperature increments in the range 25−50 °C, and the readings were taken after 3 min equilibration at each temperature.

Results and Discussion

MSN functionalized with thiol groups for linking to the modified PNIPAM polymer were synthesized by condensation of tetraethylorthosilicate with mercaptopropyl trimethoxysilane (MPTMS) in the presence of the micellar template, *N*-cetyltrimethylammonium bromide (CTAB).[3] Removal of CTAB by acid washing resulted in MSN with sizes of 80−90 nm in diameter (Figure 1a) and Braunaer−Emmett−Teller (BET) surface areas of 1500 m^2/g. The pore diameters were computed by BJH and DFT methods to be 1−4 nm (Supporting Information, Figure S4), and the BJH cumulative pore volume was 0.51 cm^3/g. X-ray powder diffraction (Figure 2) shows only a single resolved peak at $d = 4$ nm, suggesting a low degree of order in the pore structure, making assignment of hexagonal (straight pores) or cubic (wormhole interconnected pores) polymorph ambiguous. Molecular transport can occur in either structure, although it is more facile in the interconnected pore structure.[24] The accessible

(24) Walcarius, A.; Delacôte, C. *Chem. Mater.* **2003**, *15*, 4181–4192.
(25) Reiner, C. K.; Kada, G.; Gruber, H. J. *Anal. Bioanal. Chem.* **2002**, *373*, 266–276.
(26) Webb, P. A.; Orr, C. *Analytical Methods in Fine Particle Technology*; Micromeritics Instrument Corp.: Norcross, GA, 1997.
(27) Rossi, L. M.; Shi, L.; Quina, F. H.; Rosenzweig, Z. *Langmuir* **2005**, *21*, 4277–4280.
(28) Rao, K. S.; El-Hami, K.; Kodaki, T.; Matsushige, K.; Makino, K. *J. Colloid Interface Sci.* **2005**, *289*, 125–131.

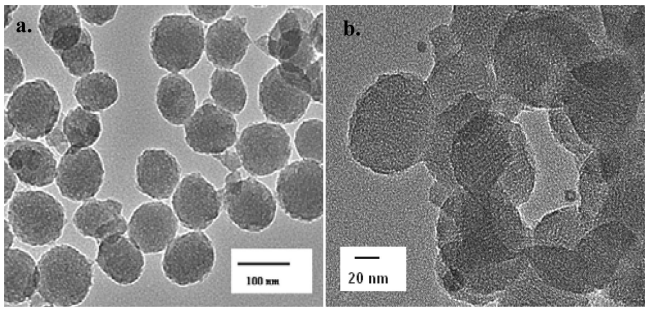

Figure 1. TEM image of (a) as-prepared mesoporous MSN-SH and (b) MSN-PNIPAM nanoparticles.

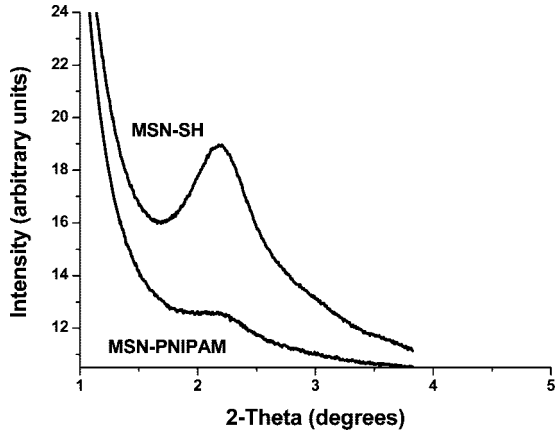

Figure 2. Low-angle PXRD pattern of MSN-SH and MSN-PNIPAM. The reduction in peak intensity for MSN-PNIPAM is attributed to decreased contrast due to the polymer.[1,32,33]

thiol content of the MSN-SH material was computed to be 6.0×10^{-4} mol/g by titration with Ellman's reagent.

The pyridyl disulfide-terminated PNIPAM polymer was synthesized in three steps (Scheme 1). First, a reversible addition-fragmentation chain transfer polymerization was employed to synthesize narrow polydispersity PNIPAM with a trithiocarbonate end group (PNIPAM−S−C(=S)−S−$C_{12}H_{25}$). The synthesized PNIPAM−S−C(=S)−S−$C_{12}H_{25}$ (M_n = 11 800, M_w/M_n = 1.12) was then treated with hexylamine at room temperature to form PNIPAM with a terminal thiol group (PNIPAM-SH). Finally, PNIPAM-SH was treated with 2,2′-dipyridyl disulfide (Aldrithiol-2) to produce pyridyl disulfide-terminated PNIPAM (PNIPAM−S−S−Py, M_n = 12 100, M_w/M_n = 1.30).

The thiol-functionalized MSN were reacted with PNIPAM−S−S−Py at room temperature to prepare the hybrids (MSN-PNIPAM) as illustrated in Scheme 2. The resultant hybrid particles show improved dispersion in water at room temperature relative to the native MSN, which we attribute to the solubilizing nature of PNIPAM. A comparison of thermal gravimetric analysis data for the hybrid, MSN-SH and PNIPAM−S−S−Py, suggests that ~20 wt % of the hybrid is due to the grafted polymer (Figure 3). FT-IR data are also consistent with a chemical linkage between MSN and PNIPAM. A comparison of FT-IR spectra of MSN-SH, MSN-PNIPAM, and PNIPAM

Scheme 2. Reaction of MSN-SH with PNIPAM−S−S−Py To Form MSN-PNIPAM

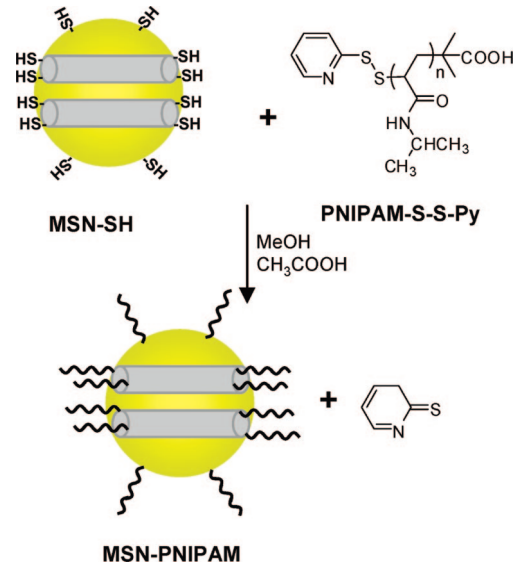

(Figure 4), shows that the two characteristic peaks for PNIPAM at 1650 (amide stretch) and 1553 cm^{-1} (N−H stretch)[29] appear in the MSN-PNIPAM but not in MSN-SH. In addition, the silica framework of MSN in MSN-PNIPAM remains unchanged upon PNIPAM grafting, as evidenced by preservation of peaks at 461, 800, and 1090 cm^{-1}, associated with silica.[30] The overall morphology and particle size also remain unchanged in MSN-PNIPAM, as shown in Figure 1, but the surface area is decreased by 2 orders of magnitude, suggesting that grafting the polymer onto MSN blocks the pores in the solid state (Supporting Information). Indeed, the extremely low surface area (23 m^2/g) and the broad, featureless pore-size distribution plot (Supporting Information) suggest that only the outer surface and voids between precipitated particles are being probed.

Loading and release studies were conducted with fluorescein as a model drug molecule. First, to demonstrate temperature-controlled uptake of small organic molecules into MSN-PNIPAM, experiments were performed with

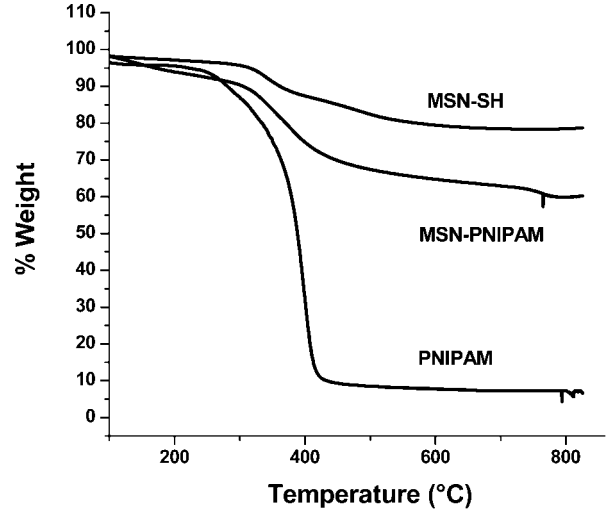

Figure 3. TGA curves for MSN-SH, MSN-PNIPAM, and PNIPAM.

(29) Xie, R.; Chu, L.-Y.; Chen, W.-M.; Xiao, W.; Wang, H.-D.; Qu, J.-B. *J. Membr. Sci.* **2005**, *258*, 157–166.
(30) Gu, G.; Ong, P. P.; Chu, C. *J. Phys. Chem. Solids* **1999**, *60*, 943–947.

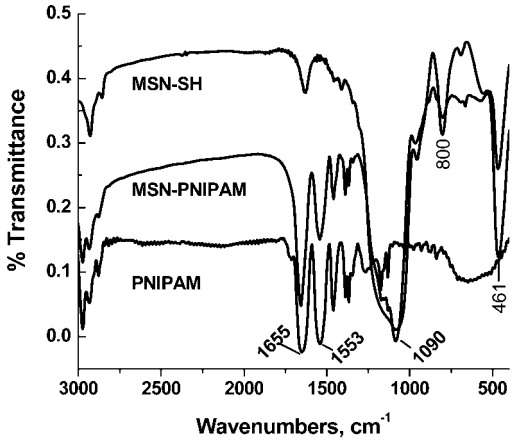

Figure 4. FT-IR spectra of MSN-SH, MSN-PNIPAM, and PNIPAM.

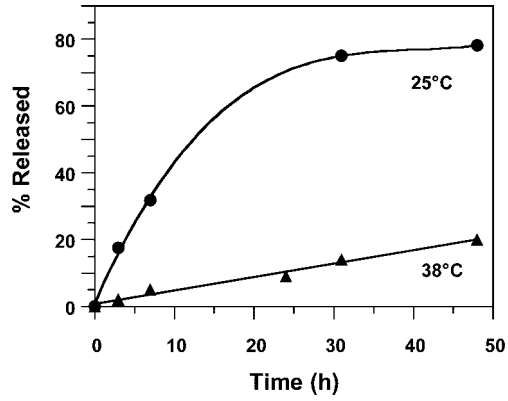

Figure 5. Relative amount of fluorescein released with time at 38 (▲) and 25 °C (●).

fluorescein (4×10^{-6} M) in phosphate-buffered saline (PBS). The MSN-PNIPAM was stirred vigorously in a solution of fluorescein at room temperature for 24 h. Then, the temperature of the solution was increased to 38 °C, and the precipitated MSN-PNIPAM was filtered, washed extensively with 50 °C PBS solution to remove fluorescein molecules adsorbed on the surface, and dried at 50 °C. The loading was performed for 24 h at temperatures above and below the LCST of PNIPAM. The results showed that no detectable amount of fluorescein could be loaded into the MSN-PNIPAM above the LCST (38 °C). Fluorescein, however, entered the MSN-PNIPAM below the LCST (25 °C). The 25 °C loaded samples contained 8×10^{-8} mol fluorescein per gram of MSN-PNIPAM. On the basis of the BJH cumulative pore volume of 0.51 cm^3/g for MSN-SH and taking into account a 20% increase in mass due to PNIPAM (computed from TGA analyses), this suggests the concentration of fluorescein within the pores is on the order of 2×10^{-5} M, similar to the fluorescein concentration in the original solution (4×10^{-6} M).

We then investigated whether, in addition to temperature-controlled loading, the MSN-PNIPAM also showed temperature-dependent release of fluorescein. The release data at 25 (below LCST) and 38 °C (above LCST) are shown in Figure 5. Similar to the loading experiments, the soluble PNIPAM chains rendered the entrances of pores open below the phase transition at 25 °C. This was demonstrated by a gradual release of the fluorescein loaded in the voids of MSN.

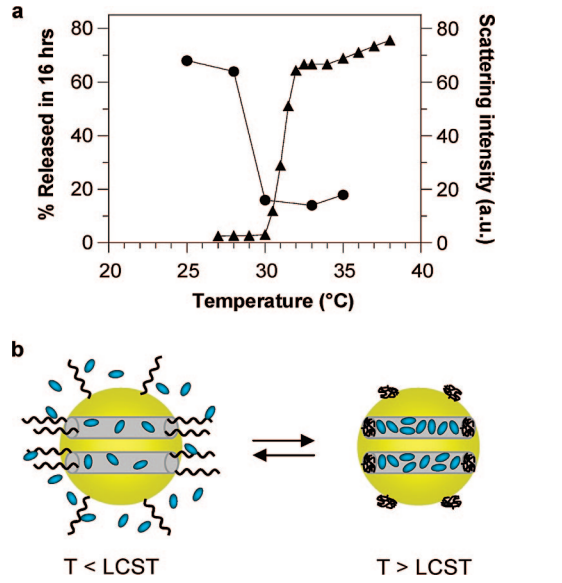

Figure 6. (a) Correlation between release of fluorescein from MSN-PNIPAM (●) and phase transition of PNIPAM (indicated by the increase of light scattering intensity) (▲). (b) Schematic representation of the principle of action.

On the other hand, PNIPAM chains are insoluble in PBS at 38 °C, the entrances of pores are blocked by the collapsed PNIPAM chains, and the release of fluorescein from the voids of MSN is significantly obstructed.

To further investigate the link between the conformation of the polymer and its pore opening/closing capability, we determined the total amount of fluorescein released in 16 h at different temperatures and compared this data to the light-scattering behavior of the polymer sample at that temperature. We expected that the transformation from the soluble, random coil conformation of PNIPAM to the insoluble, globule form would result in a blocking of the pores of the hybrid MSN-PNIPAM materials. As shown in Figure 6a, the amount of released fluorescein decreases dramatically around 30 °C, concomitant with a clear increase in scattering intensity. Thus, release of small organic molecules loaded in MSN-PNIPAM can be controlled by the phase state of the modifying PNIPAM chains. However, it appears that the polymer alone cannot act as an effective system for stimuli-responsive uptake and release. Control experiments in which the uptake was attempted with PNIPAM grafted onto dense (nonporous) silica spheres showed no evidence for fluorescein encapsulation, regardless of temperature, suggesting that the porosity of the MSN is integral to the storage of fluorescein.

The mechanism of action in the presently reported materials is clearly different from that reported by López and co-workers, where release was observed *above* LCST.[22,23] These materials were prepared by either preforming MSN and growing the PNIPAM polymer from the surface or preforming PNIPAM and co-condensing it with silica during formation of MSN. In either case, incorporation of the polymer within the pores can occur readily. Thus, contraction above LCST would be expected to effectively open the pores, while the random coil network of polymer present below LCST would be expected to act as a diffusion barrier. We surmise that the present method of synthesis, in which both

PNIPAM and MSN components are preformed, results in significant grafting at the pore surface. Thus, above LCST, the polymer forms "stoppers" that prevent uptake and release, whereas below this temperature, the random coil conformation permits diffusion into and out of the pores (Figure 6b). The presence of the polymer preferentially at the pore surface would be expected based on the significant molecular weight of the polymer ($M_n = 12\ 100$), the relatively small size of the pores (1−4 nm), and the rapid kinetics of the reaction of pyridyl disulfide with free thiol. The ability to exclude the access of molecules to mesoporous silica based on their size is a characteristic feature of these materials.[31] Although we cannot rule out the presence of polymer within the pores, the observed response strongly suggests that surface polymer dominates the temperature-dependent uptake and release.

The presence of the polymer is clearly active in moderating diffusion, as can be seen when the release profile of the unmodified MSN-SH is compared (Supporting Information). Approximately twice as much fluorescein is released after 24 h for MSN-SH than for the MSN-PNIPAM hybrid in the "open" configuration (below LCST). Indeed, diffusion into and from the pores for the present system in the "pore-open" configuration appears to be slower than that for the co-condensed materials in the "pore-closed" configuration (∼10% vs ∼30% release after 2 h); in the "pore-closed" configuration, <20% release occurs after 16 h in the new materials. Thus, application of preformed polymer to preformed porous particles appears to enable much greater control over the release.

Conclusion

The present work demonstrates that the phase state of a temperature-responsive polymer can control opening and closing of the pores when grafted onto preformed micro-to-mesoporous silica nanoparticles. Further work is underway to apply this approach to the development of porous nanoparticles in which the molecular gates around the pores are reversibly switched on and off by other stimuli, such as pH, and develop new chemical attachment strategies that will result in polymer−particle tethers that are not subject to cleavage under physiological conditions. This general approach can be used to expand the choice of stimulus-controlled drug and gene delivery systems in which a fully reversible loading and release mechanism is required.

Acknowledgment. This work was supported by NIH Grants EB0043588 and EB008164 from the National Institute of Biomedical Imaging and Bioengineering and the Institute of Manufacturing Research of Wayne State University. We thank Ingrid Zenke and Hans Riegler of the Max Planck Institute of Colloids and Interfaces for X-ray diffraction data.

Supporting Information Available: ^{1}H NMR of DMP; details on the characterization of PNIPAM-S-S-Py along with absorbance spectra and GPC trace; details on surface area analyses of MSN materials and isotherm/pore-size distribution plots; data for fluorescein release from MSN-SH (control reaction) (PDF). This material is available free of charge via the Internet at http://pubs.acs.org.

CM703363W

(31) Zapilko, C.; Anwander, R. *Chem. Mater.* **2006**, *18*, 1479–1482.
(32) Parala, H.; Winkler, W.; Kolbe, M.; Wohlfart, A.; Fischer, R. A.; Schmechel, R.; von Seggern, H. *Adv. Mater.* **2000**, *12*, 1050–1055.
(33) Zhang, W.-H.; Shi, J.-L.; Chen, H.-R.; Hua, Z.-L.; Yan, D.-S. *Chem. Mater.* **2001**, *13*, 648–654.